CSIAM Trans. Appl. Math.
doi: 10.4208/csiam-am.SO-2023-0022

Vol. **x**, No. x, pp. 1-13
xx 2024

On the Optimal Order Approximation of the Partition of Unity Finite Element Method

Yunqing Huang[1] and Shangyou Zhang[2,*]

[1] *Hunan Key Laboratory for Computation and Simulation in Science and Engineering, Xiangtan University, Hunan 411105, China.*
[2] *Department of Mathematical Sciences, University of Delaware, Newark, DE 19716, USA.*

Received 17 June 2022 ; Accepted 11 December 2023

Abstract. In the partition of unity finite element method, the nodal basis of the standard linear Lagrange finite element is multiplied by the P_k polynomial basis to form a local basis of an extended finite element space. Such a space contains the P_1 Lagrange element space, but is a proper subspace of the P_{k+1} Lagrange element space on triangular or tetrahedral grids. It is believed that the approximation order of this extended finite element is k, in H^1-norm, as it was proved in the first paper on the partition of unity, by Babuska and Melenk. In this work we show surprisingly the approximation order is $k+1$ in H^1-norm. In addition we extend the method to rectangular/cuboid grids and give a proof to this sharp convergence order. Numerical verification is done with various partition of unity finite elements, on triangular, tetrahedral, and quadrilateral grids.

AMS subject classifications: 65N15, 65N30

Key words: Finite element, partition of unity, triangular grid, tetrahedral grid, rectangular grid.

1 Introduction

The partition of unity finite element was proposed in 1996 [10]. The method is based on the P_1 Lagrange finite element

$$u_h(\mathbf{x}) = \sum_{\mathbf{v}_i \in \mathcal{V}_h} u_i \phi_i(\mathbf{x}), \tag{1.1}$$

where u_i is the nodal value of a continuous function u_h at a vertex, $u_h(\mathbf{v}_i), \mathcal{V}_h$ is the index set of vertices in a triangulation $\mathcal{T}_h$, and ϕ_i is a piecewise P_1 function on the grid $\mathcal{T}_h$ assuming value 1 at one vertex $\mathbf{v}_i$ and zero at the rest vertices. Instead of multiplied by the P_0

*Corresponding author. *Email addresses:* `huangyq@xtu.edu.cn` (Y. Huang), `szhang@udel.edu` (S. Zhang)

 ©2024 Global-Science Press

polynomial in (1.1), in one partition of unity method each nodal basis $\phi_i(\mathbf{x})$ is multiplied by the P_k polynomial basis, cf. [1,8,10],

$$u_h(\mathbf{x}) = \sum_{\mathbf{v}_i \in \mathcal{V}_h} u_i(\mathbf{x})\phi_i(\mathbf{x}), \quad u_i(\mathbf{x}) = \sum_{|\alpha| \le k} u_{i,\alpha}(\mathbf{x}-\mathbf{v}_i)^\alpha, \tag{1.2}$$

where α is a multi-index, e.g., when $k=2$ in 2D, $\mathbf{x}^\alpha \in \{1,x,y,x^2,xy,y^2\}$.

Obviously, the extended finite element space contains the P_1 Lagrange finite element as a subspace, by letting $u_i(\mathbf{x}) \in \mathbb{R}$ in (1.2). On the other side, because the sum of three P_1 basis functions at the three vertices of a triangle K is a constant function 1, the extended finite element space also contains the $P_k(K)$ Lagrange element space as a subspace locally, on this triangle K only. But globally, on a triangular grid in 2D, the dimension of $P_1 \times P_k$ finite element space (P_1 Lagrange basis multiplied by P_k polynomials) is $C(k+1)(k+2)/2 \sim Ck^2/2$ while that of P_k Lagrange finite element space is Ck^2, by the Euler formula, where C is about the number of vertices. For large k, C^0-$(P_1 \times P_k) \not\supset C^0$-$P_k$. Nevertheless, the first partition of unity paper [10] proved an $\mathcal{O}(h^k)$ H^1-convergence and an $\mathcal{O}(h^{k+1})$ L^2-convergence for this partition of unity finite element method. This is not trivial, to prove a smaller space having the same order of approximation.

We may compare the $P_1 \times P_k$ finite element space with the P_{k+1} Lagrange element space. Each extended finite element function u_h is a $p_1 \times p_k = p_{k+1}$ polynomial, on each element. The partition of unity finite element space is clearly a subspace of the P_{k+1} Lagrange space. In 1D, because the number of elements is the same as the number of vertices (one less), from a dimension counting, the extended finite element space is precisely the P_{k+1} Lagrange space in 1D. In [7] proved an one-order higher convergence than that of [10] in 1D.

But the problem is less trivial in 2D and 3D, and remains open for twenty some years. For example, for the P_2 triangular element in 2D, the finite element dimension is the sum of the number of vertices and the number of edges. For the $P_1 \times P_1$ partition of unity finite element, the space dimension is 3 times the number of vertices. By the Euler formula, the number of edges is about three times of the number of vertices. The dimension of the $P_1 \times P_1$ space is about 3/4 of that of the P_2 Lagrange space. Similarly, the dimensions of $P_1 \times P_k$ partition of unity finite element space and P_{k+1} Lagrange finite element space are about the number of vertices times $(k+1)(k+2)/2$ and $(k+1)^2$, respectively, on 2D triangular grids. For large k, the former is about half of the latter. On 3D tetrahedral grids, the dimensions of $P_1 \times P_k$ partition of unity finite element space is about the number of vertices times $(k+1)(k+2)(k+3)/6$ while that of P_{k+1} Lagrange finite element space is about the number of vertices times $(k+1)^3$. The ratio is about 1/6 for large k. These ratios become even smaller for the $Q_1 \times P_k$ partition of unity finite element space and the Q_{k+1} Lagrange finite element space, on 2D and 3D rectangular grids. We also extend this method to rectangular/cuboid grids in this paper.

Though the $P_1 \times P_k$ partition of unity finite element space is a proper subspace of the P_{k+1} Lagrange finite element space, we prove both have the same order of convergence in this paper. That is, we show that the $P_1 \times P_k$ partition of unity finite element solution converges at $\mathcal{O}(h^{k+1})$ in H^1-norm and at $\mathcal{O}(h^{k+2})$ in L^2-norm when solving the second order elliptic boundary value problems. We note that on one element the interpolation does not recover a P_{k+1} polynomial, but on a patch of elements a quasi-interpolation does recover the P_{k+1} polynomial at the central element. Because the basis functions of partition of unity finite element are supported on a larger patch of elements than that of Lagrange P_{k+1} element, the solution from a subspace, the partition of unity finite element space, could be as accurate as the solution from the whole P_{k+1} Lagrange element space. This theory is confirmed numerically. In addition, observed from numerical tests, when the solution of P_{k+1} Lagrange element is superconvergent, so is the partition of unity finite element solution.

Some influential works on the partition of unity method are [2,3,11,13].

2 The $P_1 \times P_k$ finite element

Let a polygonal or a polyhedral domain be partitioned in to a regular triangular or tetrahedral grids $\mathcal{T}_h$, of grid size h. The partition of unity $P_1 \times P_k$ finite element spaces are defined by

$$V_h = \Big\{ u_h = \sum_{\mathbf{v}_i \in \mathcal{V}_h, |\alpha| \le k} c_{i,\alpha} (\mathbf{x} - \mathbf{v}_i)^\alpha \phi_i(\mathbf{x}) \mid \phi_i \in C^0,$$

$$\phi_i|_K \in P_1(K), \phi_i(\mathbf{v}_j) = \delta_{i,j}, \forall \mathbf{v}_i, \mathbf{v}_j \in \mathcal{V}_h \Big\}, \tag{2.1}$$

$$V_h^{(0)} = \{ u_h \in V_h \mid u_h|_{\partial\Omega} = 0 \}, \tag{2.2}$$

where $K \in \mathcal{T}_h, \mathcal{V}_h$ is the set of vertices of $\mathcal{T}_h$, and α is a 2D, or 3D multi-index. We solve the following second-order elliptic equation: Find $u \in H^1(\Omega)$ such that $u|_{\partial\Omega} = g$ and

$$a(u,v) = (f,v), \quad \forall v \in H_0^1(\Omega), \tag{2.3}$$

where

$$a(u,v) = \int_\Omega (A \nabla u) \cdot \nabla v d\mathbf{x}, \quad (f,v) = \int_\Omega f v d\mathbf{x},$$

where $A = A(\mathbf{x})$ is a $d \times d$ matrix, uniformly symmetric and positive definite on Ω. The finite element approximation problem reads: Find $u_h \in V_h$ such that $u_h|_{\partial\Omega} = I_{k+1} g$ and

$$a(u_h, v_h) = (f, v_h), \quad \forall v_h \in V_h^{(0)}, \tag{2.4}$$

where I_{k+1} is the continuous P_{k+1} Lagrange interpolation on the boundary of domain Ω.

Remark 2.1. The set of spanning functions, $\{(\mathbf{x} - \mathbf{v}_i)^\alpha \phi_i(\mathbf{x}), \mathbf{v}_i \in \mathcal{V}_h, |\alpha| \le k\}$, is not linearly independent, i.e. it does not form a basis for V_h, but a frame for V_h. This can be seen if the triangulation consists of only one triangle, or one tetrahedron in 3D. In computation, if using an iterative solver such as the conjugate gradient iteration, one can simply use the linearly dependent frame (2.1). Otherwise we do an extra Gaussian elimination on the stiffness matrix to block dependent spanning functions from entering the set of basis.

3 The convergence theory

We will study an overlapping interpolation and show its optimal order of approximation. The optimal order of convergence of the finite element solution would follow as it is an optimal projection of the true solution.

We first prove a trivial lemma. Its purpose is to show a P_{k+1}-preserving map from $\mathbb{R}^{\dim P_{k+1}}$ to $[\mathbb{R}^{\dim P_k}]^d$ ($d=2,3$).

Lemma 3.1. *On a triangle or tetrahedron K,*

$$\operatorname{span}\left\{(\mathbf{x}-\mathbf{v}_i)^\alpha \phi_i(\mathbf{x}) \,|\, \mathbf{v}_i \text{ are vertices of } K, |\alpha|\le k\right\} = P_{k+1}(K). \tag{3.1}$$

Proof. We prove the case of 3D. Let $\{\mathbf{v}_i\}$ be the four vertices of K. Let $\{\lambda_1,\ldots,\lambda_4\}$ be the barycentric coordinate variables. These are linear functions satisfying $\lambda_i(\mathbf{v}_j)=\delta_{i,j}$. For any polynomial $u\in P_{k+1}(K)$, we have a unique expansion under the homogeneous barycentric polynomials

$$u=\sum_{i_1+i_2+i_3+i_4=k+1} c_{i_1i_2i_3i_4}\lambda_1^{i_1}\lambda_2^{i_2}\lambda_3^{i_3}\lambda_4^{i_4}, \tag{3.2}$$

i.e. the polynomial in barycentric coordinate variables, instead of Cartesian coordinate variables. We separate u into four functions

$$\begin{aligned} u_1&=\sum_{i_1+i_2+i_3+i_4=k+1}\frac{i_1}{k+1}c_{i_1i_2i_3i_4}\lambda_1^{i_1}\lambda_2^{i_2}\lambda_3^{i_3}\lambda_4^{i_4},\\ u_2&=\sum_{i_1+i_2+i_3+i_4=k+1}\frac{i_2}{k+1}c_{i_1i_2i_3i_4}\lambda_1^{i_1}\lambda_2^{i_2}\lambda_3^{i_3}\lambda_4^{i_4},\\ u_3&=\sum_{i_1+i_2+i_3+i_4=k+1}\frac{i_3}{k+1}c_{i_1i_2i_3i_4}\lambda_1^{i_1}\lambda_2^{i_2}\lambda_3^{i_3}\lambda_4^{i_4},\\ u_4&=\sum_{i_1+i_2+i_3+i_4=k+1}\frac{i_4}{k+1}c_{i_1i_2i_3i_4}\lambda_1^{i_1}\lambda_2^{i_2}\lambda_3^{i_3}\lambda_4^{i_4}. \end{aligned} \tag{3.3}$$

We remark that those $i_1=0$ terms vanish in u_1 above. So we can factor out a λ_1 from the sum of u_1, assuming $\lambda_1(\mathbf{v}_i)=1$, i.e. $\mathbf{v}_i$ is the first vertex of K,

$$u_1=\lambda_1\sum_{i_1+i_2+i_3+i_4=k}\tilde{c}_{i_1i_2i_3i_4}\lambda_1^{i_1}\lambda_2^{i_2}\lambda_3^{i_3}\lambda_4^{i_4}=\phi_i(\mathbf{x})p_k, \tag{3.4}$$

where

$$\tilde{c}_{i_1i_2i_3i_4}=c_{(i_1+1)i_2i_3i_4}\frac{i_1+1}{k+1}$$

and $p_k\in P_k(K)$. The P_k polynomial in (3.4) has a unique expansion under basis $\{(\mathbf{x}-\mathbf{v}_i)^\alpha\}$ which gives

$$u_1=\phi_i(\mathbf{x})\sum_{|\alpha|\le k}c_{i,\alpha}(\mathbf{x}-\mathbf{v}_i)^\alpha. \tag{3.5}$$

Similarly, u_2, u_3 and u_4 have a unique linear expansion of basis functions at the other three vertices of K, in (3.1). As

$$u = u_1 + u_2 + u_3 + u_4,$$

u is in the span. $\square$

We define an interpolation operator. Because of the non-local frame functions $(\mathbf{x}-\mathbf{v}_i)^\alpha$, similar situations happened also in [5,6,9,14–18], the interpolation operator cannot be local ($I_h u|_K$ depends on $u|_K$ only), but quasi-local, i.e. $(I_h u)|_K$ depends on $u|_{\omega_K}$, where ω_K is the union of elements which touch a vertex of K. On a mesh $\mathcal{T}_h$, we select sequentially but randomly some free elements (none of its vertices is a vertex of a selected element) until no more such an element, see Fig. 1 for an illustration. We attach each of the left-over such isolated vertices to anyone neighbor selected element. That is, the set of vertices is separated into disjoint sets

$$\mathcal{V}_h = \bigcup_{i=1}^{i_e} \{\mathcal{V}(K_i)\} \bigcup \left[\bigcup_{i=1}^{i_0} \{\mathbf{x}_i\} \right], \tag{3.6}$$

where $\mathcal{V}(K_i)$ is the set of d vertices of $K_i, i_e = 7$ and $i_0 = 3$ for the example in Fig. 1.

On each element K_i in (3.6), let $u_L \in P_{k+1}(K_i)$ be the standard Lagrange interpolation of u on the element. Using the unique decomposition method (3.2)-(3.5), we get

$$u_L|_{K_i} = \sum_{j=1}^{d+1} \phi_j(\mathbf{x}) p_j(\mathbf{x}), \tag{3.7}$$

where $\{\mathbf{x}_j\}$ are $d+1$ vertices of K_i, and p_j is a P_k polynomial. For an isolated vertex $\mathbf{x}_i$ in (3.6), let $\mathbf{x}_i$ be the first vertex of element K_0 which is or touches the neighbor element K_i of $\mathbf{x}_i$. As the interpolation has been determined at the other d vertices of K_0 by (3.7), let $p_1 \in P_k(K)$ be anyone Lagrange interpolation (with no node on face $\phi_1 = 0$) of

$$p_1(\mathbf{x}) = I_k \left(\phi_1^{-1} \left(u(\mathbf{x}) - \sum_{m=2}^{d+1} \phi_m(\mathbf{x}) p_m(\mathbf{x}) \right) \right). \tag{3.8}$$

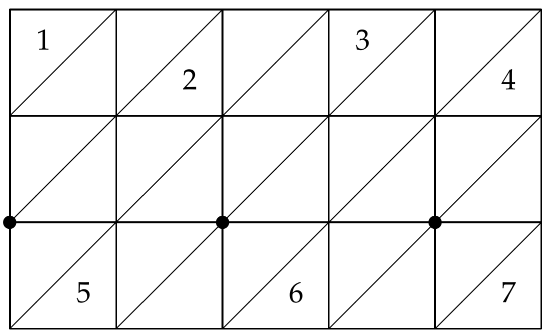

Figure 1: Selecting interpolating triangles (without mutual vertices) and three left-over nodes.

We note that if u is a one-piece P_{k+1} polynomial on a large patch which covers K_0 and all those d p_m's K_i, then the function $\phi_1^{-1}(u(\mathbf{x})-\sum_{m=2}^{d+1}\phi_m(\mathbf{x})p_m(\mathbf{x}))$ itself is a P_k polynomial. By (3.6)-(3.8), the interpolation is defined as

$$(I_h u)(\mathbf{x})=\sum_{\mathbf{x}_i\in\mathcal{V}_h}\phi_i(\mathbf{x})p_i(\mathbf{x})\in V_h. \tag{3.9}$$

Theorem 3.1. *Let $u\in H^{k+2}(\Omega)$ and $I_h u$ be defined in* (3.9). *Then*

$$\sum_{i=0}^{1}h^i\|u-I_h u\|_i\le Ch^{k+2}|u|_{k+2}. \tag{3.10}$$

Proof. As the interpolation is determined by u on a large region ω_K which includes all elements (which determine the $(d+1)$-$p_i(\mathbf{x})$) and elements in between, by the standard technique, cf. [12], we have the following interpolation stability:

$$|I_h u|_{H^1(K)}\le C|u|_{H^1(\omega_K)},$$

where C is independent of h as both regions are of size Ch. Further, if u is a one-piece P_{k+1} polynomial on whole ω_K (including those K having an left-over vertex in (3.6)),

$$(I_h u)|_K=u|_K.$$

By the above stability, the above polynomial preserving property, and the finite overlapping, following the standard argument [12], i.e. choosing an averaging Taylor polynomial $p_K\in P_{k+1}(\omega_K)$ for each $K\in\mathcal{T}_h$, we have

$$\begin{aligned}|u-I_h u|_1^2&=\sum_{K\in\mathcal{T}_h}|u-I_h u|_{H^1(K)}^2\\&\le 2\sum_{K\in\mathcal{T}_h}|u-p_K|_{H^1(K)}^2+|I_h(p_K-u)|_{H^1(K)}^2\\&\le C\sum_{K\in\mathcal{T}_h}|u-p_K|_{H^1(\omega_K)}^2\le C\sum_{K\in\mathcal{T}_h}h^{2k+2}|u|_{H^{k+2}(\omega_K)}^2\\&=Ch^{2k+2}|u|_{H^{k+2}(\Omega)}^2.\end{aligned}$$

Similarly, cf. [12], we prove the L^2 error estimate. $\square$

Theorem 3.2. *Let u and u_h be the exact solution of PDE* (2.3) *and the finite element solution of* (2.4), *respectively. Assuming the full regularity assumption* (3.11) *and $u\in H^{k+2}(\Omega)$, we have*

$$\|u-u_h\|_0+h|u-u_h|_1\le Ch^{k+2}|u|_{k+2}.$$

Proof. Noting the finite element solution u_h is the orthogonal projection of u in the inner-product $a(\cdot,\cdot)$, we have

$$\begin{aligned}|u-u_h|_1^2&\le Ca(u-u_h,u-u_h)\le Ca(u-I_h u,u-I_h u)\\&\le C|u-I_h u|_1^2\le Ch^{2k+2}|u|_{k+2}^2.\end{aligned}$$

By the standard duality argument, cf. [4], we prove the L^2 error estimate next. Let w solve the equation

$$a(w,v)=(u-u_h,v), \quad \forall v\in H_0^1(\Omega),$$

and satisfy

$$\|w\|_2\le C\|u-u_h\|_0. \tag{3.11}$$

Then we have

$$\begin{aligned}\|u-u_h\|_0^2&=a(w,u-u_h)=a(w-w_h,u-u_h)\\&\le|w-w_h|_1|u-u_h|_1\le Ch|w|_2h^{k+1}|u|_{k+2}\\&\le Ch^{k+2}|u|_{k+2}\|u-u_h\|_0.\end{aligned}$$

Canceling one $\|u-u_h\|_0$ on each side above, we obtain the L^2 estimate. □

4 The partition of unity method on rectangular and cuboid grids

Let domain Ω be partitioned into a rectangles/cuboids, noted as a set $\mathcal{T}_h$. The standard Q_1 finite element space is defined by

$$\begin{aligned}V_h^{(0)}=\Big\{u_h=\sum_{\mathbf{v}_i\in\mathcal{V}_h}c_i\phi_i(\mathbf{x})\,\big|\,\phi_i\in C^0,\phi_i|_K\in Q_1(K),\\ \phi_i(\mathbf{v}_j)=\delta_{i,j}\text{ for all vertices }\mathbf{v}_i\text{ and }\mathbf{v}_j,u_h|_{\partial\Omega}=0\Big\},\end{aligned}$$

where $K\in\mathcal{T}_h$, and $\mathcal{V}_h$ is the set of vertices of $\mathcal{T}_h$. We define $Q_1\times P_k$ partition of unity finite element space by

$$\begin{aligned}V_h=\Big\{u_h=\sum_{\mathbf{v}_i\in\mathcal{V}_h,|\alpha|\le k}c_{i,\alpha}(\mathbf{x}-\mathbf{v}_i)^\alpha\phi_i(\mathbf{x})\,\big|\,\phi_i\in C^0,\phi_i|_K\in Q_1(K),\\ \phi_i(\mathbf{v}_j)=\delta_{i,j}\text{ for all vertices }\mathbf{v}_i\text{ and }\mathbf{v}_j,u_h|_{\partial\Omega}=0\Big\},\end{aligned} \tag{4.1}$$

where α is a 2D, or 3D multi-index.

For less notations, we do the analysis in 2D only. To define an interpolation operator, we first select rectangles as before, cf. Fig. 2,

$$\mathcal{V}_h=\cup_{i=1}^{i_e}\mathcal{V}(K_i). \tag{4.2}$$

On K_1, let the standard I_hu be expressed as

$$I_hu=\sum_{i,j}c_{i,j}\phi_{i,j},$$

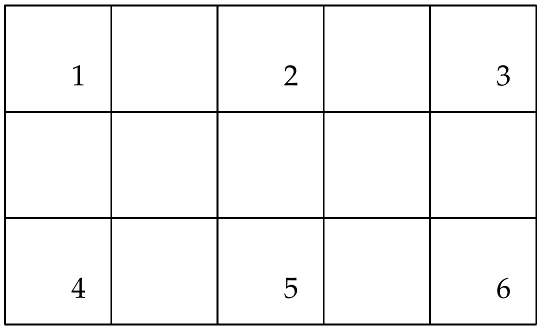

Figure 2: Selecting interpolating rectangles (no shared vertex).

where $\phi_{i,j}$ be the Q_{k+1} basis functions, i.e. on $[0,1]^2$,

$$\phi_{i,j}=\prod_{\substack{0\le i_1\le k+1,\\ i_1\neq i}}\prod_{\substack{0\le j_1\le k+1,\\ j_1\neq j}}\frac{x-i_1/(k+1)}{(i-i_1)/(k+1)}\cdot\frac{y-j_1/(k+1)}{(j-j_1)/(k+1)}.$$

Consider the decomposition,

$$\begin{aligned}
u_1&=\sum_{i,j}c_{i,j}\frac{k+1-i}{k+1}\frac{k+1-j}{k+1}\phi_{i,j}, & u_2&=\sum_{i,j}c_{i,j}\frac{i}{k+1}\frac{k+1-j}{k+1}\phi_{i,j},\\
u_3&=\sum_{i,j}c_{i,j}\frac{i}{k+1}\frac{j}{k+1}\phi_{i,j}, & u_4&=\sum_{i,j}c_{i,j}\frac{k+1-i}{k+1}\frac{j}{k+1}\phi_{i,j}.
\end{aligned}$$

Then we obtain a unique expansion of I_hu on K_1 as

$$I_hu=\sum_{i=1}^{4}p_i(\mathbf{x})\phi_i(\mathbf{x}).$$

Repeating on all i_e elements in (4.2), we define all $p_i(\mathbf{x})$ at all nodes, and we define

$$I_hu=\sum_{\mathbf{x}_i\in\mathcal{V}_h}p_i(\mathbf{x})\phi_i(\mathbf{x}). \tag{4.3}$$

We repeat the proof in last section to get the following theorems.

Theorem 4.1. *Let $u\in H^{k+2}(\Omega)$ and I_h be defined* (4.3). *Then*

$$\sum_{i=0}^{1}h^i\|u-I_hu\|_i\le Ch^{k+2}|u|_{k+2}.$$

Theorem 4.2. *Let u and u_h be the exact solution of PDE* (2.3) *and the $Q_1\times P_k$ finite element solution of* (2.4) *with V_h being defined in* (4.1), *respectively. Assuming the full regularity assumption* (3.11), *we have*

$$\|u-u_h\|_0+h|u-u_h|_1\le Ch^{k+2}|u|_{k+2}.$$

5 Numerical test

We present three numerical examples, computed on triangular grids in 2D, on square grids in 2D, and on tetrahedral grids in 3D.

5.1 Example 1. 2D triangular grids

We solve the Poisson equation with homogeneous Dirichlet boundary condition on the unit square $\Omega = (0,1)\times(0,1)$, where the exact solution is

$$u = \sin(\pi x)\sin(\pi y). \tag{5.1}$$

The grids for the computation are displayed in Fig. 3. In the Tables 1-4, we list the convergence history of the $P_1\times P_k$ partition of unity solution, in comparison with that of P_{k+1} Lagrange finite element solution, where $\tilde{I}_h$ is the nodal interpolation operator to the space of C^0-P_{k+1} finite elements. The error this way indicates superconvergence, for example, for the $P_1\times P_1$ finite element solution. The numerical order of convergence confirms the theory.

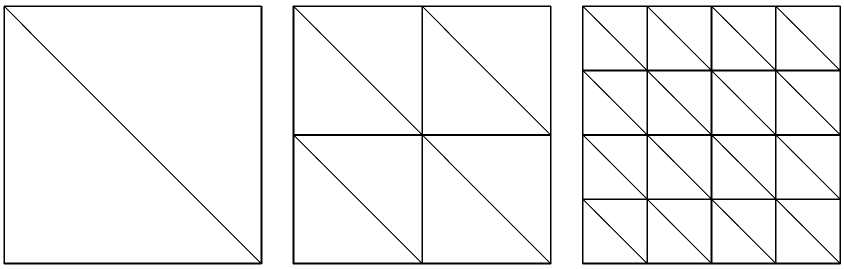

Figure 3: The first three levels of grids used in Example 1.

Table 1: The error and the numerical order of convergence (one-order superconvergent) for (5.1) (with $k=1$) on grids shown Fig. 3.

Grid	By triangular $P_1\times P_1$ partition of unity FE				
	$\|u_h-\tilde{I}_h u\|_{L^2}$	h^n	$\|u_h-\tilde{I}_h u\|_{H^1}$	h^n	$\dim V_h$
6	0.5248e-06	4.0	0.4543e-04	3.0	3267
7	0.3283e-07	4.0	0.5676e-05	3.0	12675
8	0.2053e-08	4.0	0.7094e-06	3.0	49923
9	0.1283e-09	4.0	0.8867e-07	3.0	198147
Grid	By triangular P_2 Lagrange finite element				
	$\|\tilde{u}_h-\tilde{I}_h u\|_{L^2}$	h^n	$\|\tilde{u}_h-\tilde{I}_h u\|_{H^1}$	h^n	$\dim \tilde{V}_{h,2}$
6	0.5481e-06	4.0	0.5806e-04	3.0	4225
7	0.3436e-07	4.0	0.7320e-05	3.0	16641
8	0.2150e-08	4.0	0.9187e-06	3.0	66049
9	0.1347e-09	4.0	0.1151e-06	3.0	263169

Table 2: The error and the numerical order of convergence for (5.1) (with $k=2$) on grids shown Fig. 3.

Grid	By triangular $P_1\times P_2$ partition of unity FE				
	$\|u_h-\tilde{I}_hu\|_{L^2}$	h^n	$\|u_h-\tilde{I}_hu\|_{H^1}$	h^n	$\dim V_h$
5	0.6348e-06	4.1	0.6844e-04	3.0	1734
6	0.3913e-07	4.0	0.8504e-05	3.0	6534
7	0.2435e-08	4.0	0.1061e-05	3.0	25350
8	0.1520e-09	4.0	0.1326e-06	3.0	99846
Grid	By triangular P_3 Lagrange finite element				
	$\|\tilde{u}_h-\tilde{I}_hu\|_{L^2}$	h^n	$\|\tilde{u}_h-\tilde{I}_hu\|_{H^1}$	h^n	$\dim \tilde{V}_{h,3}$
5	0.1343e-05	4.1	0.2061e-03	3.1	2401
6	0.8325e-07	4.1	0.2569e-04	3.0	9409
7	0.5180e-08	4.0	0.3205e-05	3.0	37249
8	0.3229e-09	4.0	0.4003e-06	3.0	148225

Table 3: The error and the numerical order of convergence for (5.1) (with $k=3$) on grids shown Fig. 3.

Grid	By triangular $P_1\times P_3$ partition of unity FE				
	$\|u_h-\tilde{I}_hu\|_{L^2}$	h^n	$\|u_h-\tilde{I}_hu\|_{H^1}$	h^n	$\dim V_h$
3	0.2261e-04	5.3	0.8161e-03	4.5	250
4	0.6963e-06	5.0	0.4743e-04	4.1	810
5	0.2171e-07	5.0	0.2911e-05	4.0	2890
6	0.6778e-09	5.0	0.1811e-06	4.0	10890
Grid	By triangular P_4 Lagrange finite element				
	$\|\tilde{u}_h-\tilde{I}_hu\|_{L^2}$	h^n	$\|\tilde{u}_h-\tilde{I}_hu\|_{H^1}$	h^n	$\dim \tilde{V}_{h,4}$
3	0.2455e-04	5.4	0.1135e-02	4.3	289
4	0.7786e-06	5.2	0.7157e-04	4.2	1089
5	0.2444e-07	5.1	0.4480e-05	4.1	4225
6	0.7644e-09	5.1	0.2800e-06	4.0	16641

Table 4: The error and the numerical order of convergence for (5.1) (with $k=4$) on grids shown Fig. 3.

Grid	By triangular $P_1\times P_4$ partition of unity FE				
	$\|u_h-\tilde{I}_hu\|_{L^2}$	h^n	$\|u_h-\tilde{I}_hu\|_{L^2}$	h^n	$\dim V_h$
3	0.2340e-05	5.7	0.1157e-03	4.7	375
4	0.3173e-07	6.2	0.3351e-05	5.1	1215
5	0.4508e-09	6.1	0.1017e-06	5.0	4335
6	0.6917e-11	6.0	0.3199e-08	5.0	16335
Grid	By triangular P_5 Lagrange finite element				
	$\|\tilde{u}_h-\tilde{I}_hu\|_{L^2}$	h^n	$\|\tilde{u}_h-\tilde{I}_hu\|_{H^1}$	h^n	$\dim \tilde{V}_{h,5}$
3	0.1492e-05	6.3	0.8012e-04	5.3	441
4	0.2362e-07	6.2	0.2495e-05	5.2	1681
5	0.3691e-09	6.1	0.7770e-07	5.1	6561
6	0.5673e-11	6.1	0.2452e-08	5.0	25921

5.2 Example 2. 2D square grids

We solve the Poisson equation with homogeneous Dirichlet boundary condition on the unit square $\Omega=(0,1)\times(0,1)$, where the exact solution is defined in (5.1). The grids for the computation are displayed in Fig. 4. In Table 5, we list the convergence history of the $Q_1\times P_k$ partition of unity solution. We do not have an explicit proof for the $Q_1\times P_k$ partition of unity method on square grids. But it could be similar to that of $P_1\times P_k$. The numerical order of convergence confirms this. It is interesting to note that the proof for $Q_1\times Q_k$ elements can be very similar to the proof here. But the method is deteriorated to the standard Q_{k+1} method, in 2D and 3D, and in 1D (proved in [7]).

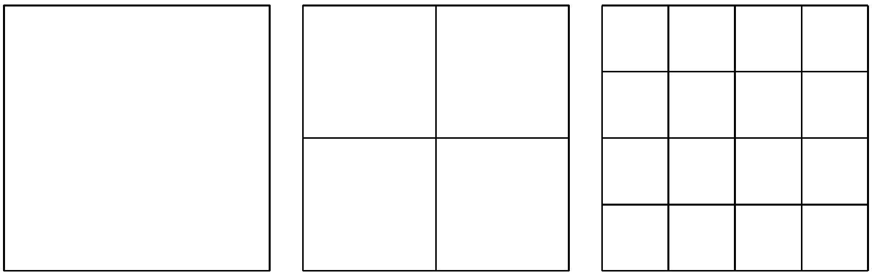

Figure 4: The first three levels of grids used in Example 2.

Table 5: The error and the order of convergence for (5.1), on 2D rectangular grids, where $\tilde{I}_h$ is the Q_{k+1} Lagrange interpolation.

Grid	$\Vert u_h-\tilde{I}_hu\Vert_{L^2}$	h^n	$\vert u_h-\tilde{I}_hu\vert_{H^1}$	h^n
	By square $Q_1\times P_1$ partition of unity FE			
5	0.4823e-04	3.2	0.2684e-02	2.1
6	0.6034e-05	3.1	0.6696e-03	2.1
7	0.7544e-06	3.0	0.1673e-03	2.0
	By square $Q_1\times P_2$ partition of unity FE			
4	0.1051e-04	4.4	0.6560e-03	3.3
5	0.6538e-06	4.2	0.8118e-04	3.1
6	0.4082e-07	4.1	0.1012e-04	3.1
	By square $Q_1\times P_3$ partition of unity FE			
3	0.9326e-05	5.9	0.4381e-03	4.8
4	0.2756e-06	5.4	0.2593e-04	4.4
5	0.8451e-08	5.2	0.1597e-05	4.2
	By square $Q_1\times P_4$ partition of unity FE			
1	0.2079e-02		0.3576e-01	
2	0.3137e-04	7.4	0.9976e-03	6.3
3	0.3957e-06	7.0	0.2660e-04	5.8

5.3 Example 3. 3D tetrahedral grids

We solve the Poisson equation with homogeneous Dirichlet boundary condition on the unit cube $\Omega=(0,1)\times(0,1)\times(0,1)$, where the exact solution is defined by

$$u(x,y,z)=\sin(\pi x)\sin(\pi y)\sin(\pi z). \tag{5.2}$$

The grids for the computation are displayed in Fig. 5. In Table 6, we list the convergence history of the $P_1\times P_k$ partition of unity solution. The numerical order of convergence confirms the theory. We note that, as for the P_2 Lagrange finite element, we also have one order of superconvergence for the tetrahedral $P_1\times P_1$ partition of unity finite element. Such a superconvergence phenomenon is not analyzed in this manuscript.

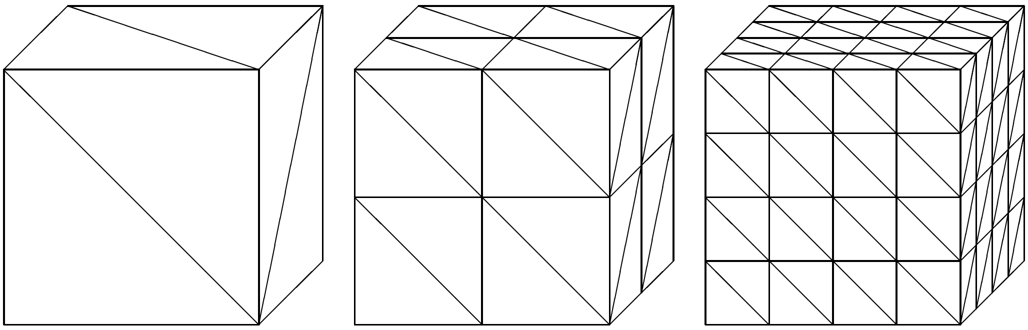

Figure 5: The first three levels of grids used in Example 3.

Table 6: The error and the order of convergence for (5.2), on 3D tetrahedral grids show in Fig. 5, where $\tilde{I}_h$ is the P_{k+1} Lagrange interpolation.

Grid	$\|u_h-\tilde{I}_h u\|_{L^2}$	h^n	$\|u_h-\tilde{I}_h u\|_{H^1}$	h^n
	By tetrahedral $P_1\times P_1$ partition of unity FE			
4	0.0002734	3.4	0.0063318	2.8
5	0.0000191	3.8	0.0008149	3.0
6	0.0000012	4.0	0.0001033	3.0
	By tetrahedral $P_1\times P_2$ partition of unity FE			
3	0.0003270	4.2	0.0106771	3.0
4	0.0000235	3.8	0.0015859	2.8
5	0.0000016	3.9	0.0002124	2.9
	By tetrahedral $P_1\times P_3$ partition of unity FE			
2	0.0015049	3.2	0.0307538	2.9
3	0.0000531	4.8	0.0021201	3.9
4	0.0000017	5.0	0.0001198	4.1

Acknowledgments

Yunqing Huang was supported in part by the NSFC Project (11971410) and by the China's National Key R&D Programs (2020YFA0713500).

References

[1] I. Babuška and J. M. Melenk, *The partition of unity method*, Int. J. Numer. Methods Eng., 40:727–758, 1997.

[2] C. Bacuta, J. Chen, Y. Huang, J. Xu, and L. Zikatanov, *Partition of unity method on nonmatching grids for the Stokes problem*, J. Numer. Math., 13(3):157–169, 2005.

[3] C. Bacuta, J. Sun, and C. Zheng, *Partition of unity refinement for local approximation*, Numer. Methods Partial Differential Equations, 27(4):803–817, 2011.

[4] S. C. Brenner and L. R. Scott, *The Mathematical Theory of Finite Element Methods*, Springer-Verlag, 1994.

[5] J. Hu, Y. Huang, and S. Zhang, *The lowest order differentiable finite element on rectangular grids*, SIAM J. Numer. Anal., 49(4):1350–1368, 2011.

[6] J. Hu, S. Zhang, and Z. Zhang, *On the* $2p$*th-order of convergence of the Galerkin finite difference method*, SIAM J. Numer. Anal., 57(5):2189–2199, 2019.

[7] Y. Huang, W. Li, and F. Su, *Optimal error estimates of the partition of unity method with local polynomial approximation spaces*, J. Comput. Math., 24(3):365–372, 2006.

[8] Y. Huang and J. Xu, *A conforming finite element method for overlapping and nonmatching grids*, Math. Comp., 72(243):1057–1066, 2003.

[9] Y. Huang and S. Zhang, *Supercloseness of the divergence-free finite element solutions on rectangular grids*, Commun. Math. Stat., 1(2):143–162, 2013.

[10] J. M. Melenk and I. Babuška, *The partition of unity finite element method: Basic theory and applications*, Comput. Methods Appl. Mech. Eng., 139(1-4):289–314, 1996.

[11] J. M. Melenk and I. Babuška, *Approximation with harmonic and generalized harmonic polynomials in the partition of unity method*, Comput. Assist. Mech. Eng. Sci., 4:607–632, 1997.

[12] L. R. Scott and S. Zhang, *Finite-element interpolation of non-smooth functions satisfying boundary conditions*, Math. Comp., 54:483–493, 1990.

[13] T. Strouboulis, I. Babuška, and K. Copps, *The design and analysis of the generalized finite element method*, Comput. Methods Appl. Mech. Eng., 181(1-3):43–69, 2000.

[14] S. Zhang, *A C1-P2 finite element without nodal basis*, ESAIM Math. Model. Numer. Anal., 42:175–192, 2008.

[15] S. Zhang, *A family of* $Q_{k+1,k}\times Q_{k,k+1}$ *divergence-free finite elements on rectangular grids*, SIAM J. Numer. Anal. 47(3):2090–2107, 2009.

[16] S. Zhang, *On the full* C_1-Q_k *finite element spaces on rectangles and cuboids*, Adv. Appl. Math. Mech., 2(6):701–721, 2010.

[17] S. Zhang, *Quadratic divergence-free finite elements on Powell-Sabin tetrahedral grids*, Calcolo, 48(3):211–244, 2011.

[18] S. Zhang, Z. Zhang, and Q. Zou, *A postprocessed flux conserving finite element solution*, Numer. Methods Partial Differential Equations, 33(6):1859–1883, 2017.